JACS
JOURNAL OF THE AMERICAN CHEMICAL SOCIETY
Communication
pubs.acs.org/JACS

Direct Observation of Large Quantum Interference Effect in Anthraquinone Solid-State Junctions

Vincent Rabache,[†] Julien Chaste,[†] Philippe Petit,[†] Maria Luisa Della Rocca,[†] Pascal Martin,[§] Jean-Christophe Lacroix,[§] Richard L. McCreery,[‡] and Philippe Lafarge*[,†]

[†]Université Paris Diderot, Sorbonne Paris Cité, MPQ, UMR 7162 CNRS, 75205 Paris Cedex 13, France
[§]Université Paris Diderot, Sorbonne Paris Cité, ITODYS, UMR 7086 CNRS, 75205 Paris Cedex 13, France
[‡]National Institute for Nanotechnology, University of Alberta, Edmonton, Alberta Canada, T6G 2M9

Supporting Information

ABSTRACT: Quantum interference in cross-conjugated molecules embedded in solid-state devices was investigated by direct current−voltage and differential conductance transport measurements of anthraquinone (AQ)-based large area planar junctions. A thin film of AQ was grafted covalently on the junction base electrode by diazonium electroreduction, while the counter electrode was directly evaporated on top of the molecular layer. Our technique provides direct evidence of a large quantum interference effect in multiple CMOS compatible planar junctions. The quantum interference is manifested by a pronounced dip in the differential conductance close to zero voltage bias. The experimental signature is well developed at low temperature (4 K), showing a large amplitude dip with a minimum >2 orders of magnitude lower than the conductance at higher bias and is still clearly evident at room temperature. A temperature analysis of the conductance curves revealed that electron−phonon coupling is the principal decoherence mechanism causing large conductance oscillations at low temperature.

Understanding and controlling electronic transport through molecular layers is one of the main goals of molecular electronics. Many different effects are used to tune the transport properties of molecular devices. One such method, quantum interference in cross conjugated molecules, results in the drastic but reversible reduction of the conductance in molecular devices. Quantum interference results from the wave properties of electrons and is a well-known quantum effect in mesoscopic physics.[1−3] The ability to control quantum interference at the molecular level could improve knowledge of electron transport through molecular systems and provide novel electronic behavior of molecular junctions. Furthermore, the nanometric size of a molecular system implies large energy scales, making it possible to address quantum effects at room temperature (rt). Consequently, quantum interference in molecules has recently attracted great interest, both theoretically[4−14] and experimentally.[15−20]

One of the first molecular systems where these effects have been predicted is a benzene ring connected to two metallic leads in a meta configuration.[4−6,10] Generally, such effects are predicted to occur with specific unsaturated molecules, i.e., cross-conjugated molecules. Such systems are composed of three unsaturated groups, two of which are conjugated to the third but not conjugated to each other.[9,14] A recent theoretical report presents an elegant and simple graphical method to predict the occurrence of interference effects in single molecules by considering the molecular structure and its bonding to electrodes.[12] The anthraquinone (AQ) molecule, whose diazonium derivative is shown in Figure 1b (top), is of particular

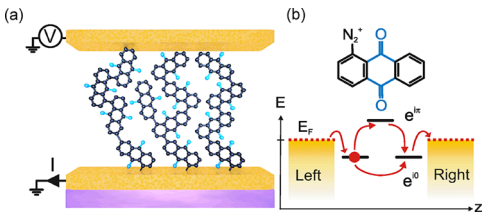

Figure 1. (a) Simplified scheme of the planar junction based on an AQ layer covalently grafted on the bottom electrode. (b) Structure of the diazonium derivative of the AQ molecule before grafting (top). Three-level scheme showing the electron pathways through the molecular orbitals interfering destructively according to ref 12 (bottom).

interest, because it is intrinsically cross-conjugated as long as contact between the bottom and top electrodes involves the two peripheral aromatic rings. Indeed, these molecules are comprised of three unsaturated rings, with the central quinone unit (blue in Figure 1b) conjugated to each of the unsaturated peripheral benzene rings, but with these two benzene rings not conjugated to each other. Quantum interference has recently been explored experimentally in AQ and related molecules[16−20] molecular junctions.

The expected signature of quantum interference in transport through a molecule is a reduction of the transmission resulting from destructive interference, with a clear antiresonance[9−14,17] at the energy where interference occurs. A simple model for the AQ junctions is shown in Figure 1b (bottom) representing localized molecular orbitals of the three subunits of the molecule. An electron transported from the left to the right electrode can follow two distinct paths, represented by the arrows in Figure 1b (bottom), thus leading to the destructive interference for this case. According to theory, the ideal system for observing

Received: April 10, 2013
Published: June 27, 2013

   dx.doi.org/10.1021/ja403577u | J. Am. Chem. Soc. 2013, 135, 10218−10221

quantum interference is a single molecule junction based on a cross-conjugated system.[12] This has been demonstrated recently[18,19] but requires the ability to realize electrodes spaced very closely together (~nm) and bonded to opposite ends of a single molecule. Although significant progress has been made in realizing nanogaps (i.e., electromigration,[21−23] with controllable break junctions,[24,25] and electrochemical methods[26]), reproducible fabrication of identical single molecule devices is still far from possible. Consequently, most experimental reports rely on statistical analysis of a large number of single molecule junctions to observed conductance differences. Recently, quantum interference effects have also been reported in systems involving more than single molecules. Guedon et al.[17] observed transport measurements on metal−molecule−metal junctions consisting of ~100 AQ molecules contacted by a conducting AFM tip. They show not only a conductance reduction at low bias but also point out that the 2D histograms of differential conductance calculated from the current voltage characteristics have a shape that is attributed to quantum interference effects.

We investigated quantum interference on AQ molecular layers embedded in large-area, CMOS compatible solid-state devices and, for the first time, found direct experimental evidence of a large quantum interference effect through measurement of the differential conductance. Our fabrication process combines diazonium electroreduction, optical lithography, and metal evaporation We demonstrate that quantum interferences are present at rt and are enhanced as temperature is lowered for molecular films thicker than a monolayer. Furthermore, we report on the experimental signature of the electron−phonon coupling appearing at low temperature as the major source of decoherence, extinguishing interference effects. The visibility and robustness of this quantum effect on such a large area junction confirm the dominant intramolecular charge transport mechanism occurring in the molecular layer, and it paves the way for the development of practical devices based on the control of the coherent electron transport through conjugated systems and compatible with current microelectronic manufacturing.

Junctions were made using conventional fabrication techniques (see Supporting Information, SI) in cross-bar geometry.[27] Junction area ranges from 5 × 5 to 75 × 75 μm^2, with a set of larger junctions (240 × 500 μm^2) used as control experiments and reported in SI. A schematic of the junction is shown in Figure 1a. The bottom and top electrodes are made of a 2 nm Ti/50 nm Au bilayer. The few nm Ti layers are necessary to improve Au adhesion on the Si/SiO_2 substrate and reduce diffusion of Au atoms through the molecular layer. Further details of the fabrication process are found in ref 28. The AQ layer is grafted by the electroreduction of the corresponding diazonium salt.[29−32] This method ensures the formation of thin layers bonded covalently to the surface in a reproducible way, allowing a strong coupling to the electrode (details are found in the SI, along with an electrochemical characterization of the deposited layer leading to a surface concentration of 2.1 × 10^{-9} mol·cm^{-2}). The thickness of the molecular layer was estimated by measuring the cross section of the bottom electrode before and after grafting by AFM and profilometry,[33] resulting in a mean value of 5.0 ± 0.8 nm. By considering that the AQ length is ~1 nm, this implies a molecular layer containing ~5 units along the chain and is consistent with measured surface concentration. The use of ultrathin layers consisting of oligo(AQ) chains longer than the monolayer should, in theory, improve the visibility of interferences.[34] Indeed, authors in ref 34 showed that an increased length due to a larger number of cross-conjugated units has a larger effect on the amplitude of the transmission dip than an increased length obtained by adding linear conjugated units to a cross-conjugated core. Transport measurements were performed at rt and in liquid helium (4 K) and consist of differential conductance curves as a function of the applied voltage ($I(V)$ and $dI/dV(V)$). A two terminal transport measurement scheme was adopted since connection line resistance is negligible with respect to the junction resistance. The conductance (dI/dV) was measured using standard lock-in techniques with ~10 mV of excitation and a voltage bias V applied to the junction's top electrode and the bottom electrode grounded through a low impedance current amplifier. Typical current densities at 0.5 V and 4 K are in the order of 10^{-3}−10^{-4}A/cm^2.

Figure 2 shows the $I(V)$ (a) and $dI/dV(V)$ (b) curves for a 30 × 30 μm^2 area junction measured at 300 K (black circles) in

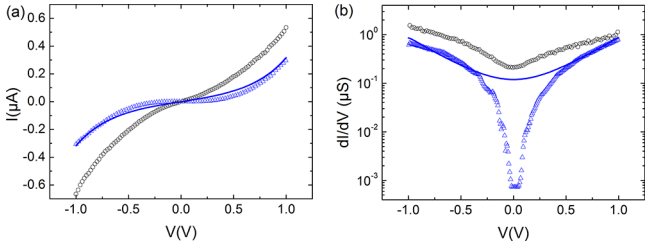

Figure 2. Measured $I(V)$ (a) and $dI/dV(V)$ (b) data for an AQ-based junction at 300 K (black circles) and 4 K (blue triangles) with an area of 30 × 30 μm^2. The solid blue line, showing a clear mismatch, is a fit of the data at 4 K to the Simmons model yielding 2.56 eV and 1.2 nm for the tunneling barrier and thickness, respectively.

comparison with the corresponding measurement at 4 K (blue triangles) in the case of an AQ molecular layer. Curves are plotted on a log-scale to illustrate the factor of ~1000 change in conductance with temperature.

A suppression of the differential conductance close to zero voltage with a typical antiresonant shape and a negative curvature is evident at rt. This shape, previously reported by Guedon et. al,[17] is the typical signature of quantum interference. Consequently, the conductance "dip" strongly suggests that destructive quantum interference is occurring in the large area AQ-based devices studied here. At 4 K, the amplitude of the dip in the differential conductance at 0 V increases to 3 orders of magnitude and also exhibits a factor of 10^3 increase in conductance between 0.01−1 V. Note that the conductance level of the points very close to zero bias is limited by the sensitivity of the acquisition instruments used during the measurement. The values of the tunneling barrier and thickness, 2.56 eV and 1.2 nm, obtained by fitting the data at 4 K to a coherent tunneling model based on the Simmons derivation[35,36] (continuous blue line in Figure 2) are inconsistent with the experimental values, and we can clearly see how the resulting curve does not match the experimental result, especially close to zero bias. Coherent tunneling should produce a parabolic curve in the log plot of the differential conductance, with no marked minimum at zero bias. Such a large temperature effect in the conductance dip at low bias is thus consistent with quantum interference effects. It is explained by considering first that decoherence is reduced when the temperature is lowered[19] and second that transport is sensitive to the thermal broadening of the Fermi function due to the variation in energy of the transmission function over several orders of magnitude, as

follows: Assuming transport is well described by the Landauer formalism, the current $I(V)$ depends on the product $T(E)$ $(f_L(E,V) - f_R(E,V))$, where $T(E)$ is the transmission probability for an electron with energy E and $f_{L(R)}$ is the Fermi functions for the left (right) electrodes. Thus, if the transmission is constant or weakly dependent on the energy, the effect of the temperature through the variation of the Fermi functions is weak. But when the transmission is strongly varying at low energy, as predicted when quantum interference occurs, a large conductance variation between rt and 4 K, as those observed here, is predicted. In mesoscopic systems, conductance suppression at zero voltage can also be related to dynamic Coulomb blockade (DCB).[37] This effect is the result of inelastic tunneling of electrons through a tunnel junction by excitation of an electromagnetic mode in the environment. Two arguments exclude such possibility in our case: First the visibility of DCB depends on the resistive and capacitive environment of the junction which has to be well controlled. In particular the resistance in the close proximity of the tunnel junction has to be of the order of the resistance quantum (12.9 kΩ), while our connection lines are large enough to show only a few ohms resistance. Moreover the large voltage range on which conductance suppression is observed on AQ-junctions implies, according to DCB theory, very low capacitance values (<0.1 aF) much lower than the capacitance of our junctions (~1 pF).

As a consequence, the specific behavior observed here strongly suggests that quantum interference effects are observed in large area solid-state molecular devices.

Figure 3 shows a magnified view of the $dI/dV(V)$ data in the temperature range $6 < T < 170$ K and in the range of $-0.3 < V <$ 0.3 V, which reveals the presence of reproducible oscillations in the conductance with magnitudes well above the noise level of the measurement. Such oscillations were observed in ~70% of the measured samples and always at low temperature and at similar bias values. Oscillations in the conductance are quite clear below 60 K, although they vanish for higher temperatures. At temperatures of ~170 K or higher, no oscillations occur but a definite minimum in the conductance plot is always present. The temperature behavior of our AQ based planar junction is consistent with recent experimental results obtained in mechanically controlled break junctions based on different types of conjugated systems,[19] where a clear temperature dependence of the junction current was detected only in the case of molecular systems for which destructive quantum interference occurs. A qualitative interpretation of the observed oscillations is based on the framework of a recent theoretical work.[38] Authors of ref 38 pointed out that quantum interferences in electron tunneling through quasidegenerate molecular states are suppressed by electron−phonon coupling, which is expected to be strong in organic systems. During tunneling electrons can lose energy by exciting a vibrational mode of the junction molecules resulting in an inelastic process. In this picture, vibrational coupling is a source of decoherence for the systems at low temperature, thus reducing interference effects. The coupling to vibrational modes is revealed by a succession of steps in the $I(V)$ characteristic of the junction at voltages given by $V_n = 2(\varepsilon + n\hbar\nu)$, where ε is the renormalized electronic state of the molecular structure, $\hbar$ the Planck constant, ν the frequency of the vibrational mode, and n an integer. As a result, peaks in the differential conductance are expected at the same voltage values. If differential conductance oscillations are actually related to the excitation of vibrational modes, they should be symmetric with respect to zero voltage. In Figure 3b we extract the $dI/dV(V)$ measurement at low temperature (6 K) where the oscillations are most pronounced.

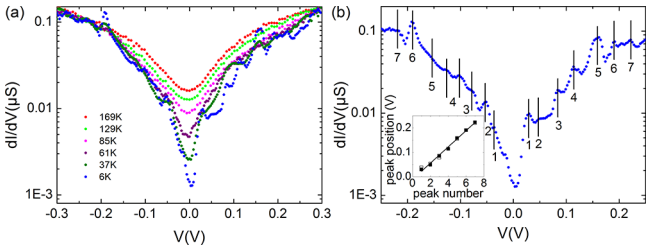

Figure 3. (a) The $dI/dV(V)$ data for an AQ junction with an area of 75 × 75 μm^2 for temperatures ranging from 6−300 K (from the bottom to the top); and (b) $dI/dV(V)$ data at 6 K: numbered vertical bars indicate the position of peaks that appears symmetrically with respect to zero voltage. Inset: linear fit to peak position vs peak number.

We numbered the peaks symmetrically with respect to zero bias in Figure 3b. If two successive peaks are associated to the same vibrational mode, their voltage separation is directly the quantity $2\hbar\nu$. From the slope of a linear fit to the peak position vs peak number shown in the inset of Figure 3b, we extract an average peak spacing of ~33 meV. The corresponding vibrational energy is in the order of 133 cm^{-1}. Such vibrational energies have been reported in many devices based on molecular systems[39] and do not seem to be specific to AQ moieties. The exact attribution in terms of molecular vibration remains an open question.

We also conducted additional transport measurements on molecular junctions made with azobenzene, a linearly conjugated molecule, and using another electrode material than Au (see SI). In that case, the $dI/dV(V)$ curve has a parabola-like shape, and we observe no conductance anomaly that is related to quantum interference. Finally, we checked the reproducibility and the robustness of the QI behavior reported here. Figure 4 shows $dI/dV(V)$ data for AQ-based junction with various areas ranging from 10 × 10 to 75 × 75 μm^2 area at rt. The four devices show very similar behavior with a typical antiresonant shape and a negative curvature which is the clear signature of quantum interference. Similar results as those reported in Figure 3 for temperatures ranging from 6−300 K were observed for the four devices. Optimization of the fabrication and grafting procedure

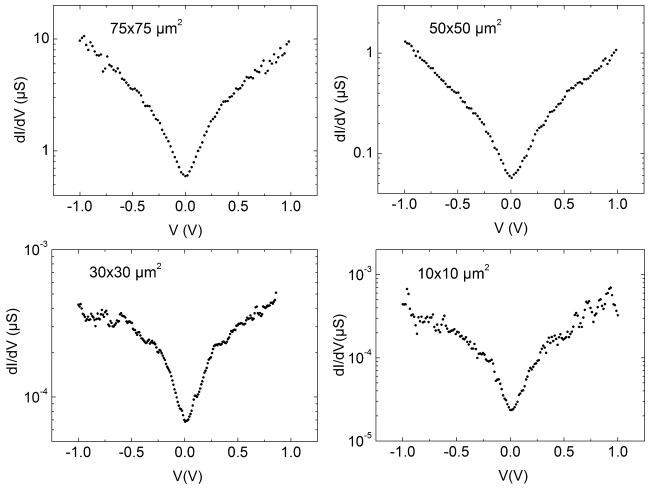

Figure 4. For four different Au/AQ/Au junctions, dI/dV measured at rt. Areas are 75 × 75, 50 × 50, 30 × 30, and 10 × 10 μm^2, respectively.

dx.doi.org/10.1021/ja403577u | J. Am. Chem. Soc. 2013, 135, 10218−10221

led to a 90% yield of junctions showing such quantum interference features.

In summary, we directly measured the differential conductance of AQ-based large area planar junctions fabricated by CMOS compatible processes. Our charge transport data on cross conjugated AQ derivatives are fully consistent with destructive quantum interference. Indeed, we show that even on large area devices containing $>10^7$ molecules, the characteristic signature of quantum interference, i.e., a dip at zero bias, is present. A temperature analysis of the differential conductance dip reveals that the amplitude of the antiresonance gains 3 orders of magnitude by cooling the system to 4 K. Furthermore we report experimentally the presence of differential conductance oscillations that is attributed to electron−phonon coupling and emerge as one of the major sources of decoherence at low temperature. Moreover, the visibility and robustness of this effect on such large area junction with inherently disordered molecular layers thicker than a monolayer indicates that charge transport is mainly intramolecular.

The observation of quantum interference effects at rt in devices generated using grafting processes and fabrication techniques compatible with current microelectronic manufacturing opens the route for implementation of devices based on quantum transport at molecular level.

■ ASSOCIATED CONTENT

Supporting Information

Grafting details and characterization data. This material is available free of charge via the Internet at http://pubs.acs.org.

■ AUTHOR INFORMATION

Corresponding Author

philippe.lafarge@univ-paris-diderot.fr

Notes

The authors declare no competing financial interest.

■ ACKNOWLEDGMENTS

We thank C. Guédon, Dr. S. J. van der Molen, and Dr. T. Markussen for helpful discussions and Dr. Haijun Yan for providing the carbon/AQ/Cu. This work is supported by ANR grant no. ANR-08-BLAN-0186-03 by C'Nano IdF, Délégation Générale de l'Armement, and Labex SEAM. Commissariat à l'investissement d'avenir and ANR are acknowledged for their financial support to labex SEAM.

■ REFERENCES

(1) Nazarov, Y. V.; Blanter, Y. *Quantum Transport: Introduction to Nanoscience*, Cambridge University Press: Cambridge, 2009.

(2) Webb, R. A.; Washburn, S.; Umbach, C. P.; Laibowitz, R. B. *Phys. Rev. Lett.* **1985**, *54*, 2696.

(3) Stone, A. D. *Phys. Rev. Lett.* **1985**, *54*, 2692.

(4) Sautet, P.; Joachim, C. *Chem. Phys. Lett.* **1988**, *153*, 511.

(5) Patoux, C.; Coudret, C.; Launay, J. P.; Joachim, C.; Gourdon. *Inorg. Chem.* **1997**, *36*, 5037.

(6) Stadler, R.; Ami, S.; Forshaw, M.; Joachim, C. *Nanotechnology* **2004**, *15*, S115.

(7) Walter, D.; Neuhauser, D.; Baer, R. *Chem. Phys.* **2004**, *299*, 139.

(8) Cardamone, D. M.; Stafford, C. A.; Mazumdar, S. *Nano Lett.* **2006**, *6*, 2422.

(9) Solomon, G. C.; Andrews, D. Q.; Goldsmith, R. H.; Hansen, T.; Wasielewski, M. R.; Van Duyne, R. P.; Ratner, M. A. *J. Am. Chem. Soc.* **2008**, *130*, 17301.

(10) Darau, D.; Begemann, G.; Donarini, A.; Grifoni, M. *Phys. Rev. B* **2009**, *79*, 235404.

(11) Solomon, G. C.; Herrmann, C.; Hansen, T.; Mujica, V.; Ratner, M. A. *Nat. Chem.* **2010**, *2*, 223.

(12) Markussen, T.; Stadler, R.; Thygesen, K. S. *Nano Lett.* **2010**, *10*, 4260.

(13) Markussen, T.; Schiötz, J.; Thygesen, K. S. *J. Chem. Phys.* **2010**, *132*, 224104.

(14) Solomon, G. C.; Andrews, D. Q.; Ratner, M. A. Quantum Interference in Acyclic Molecules. In *Charge and Exciton Transport through Molecular Wires*, Siebbeles, L. D. A., Grozema, F. C., Eds.; Wiley-VCH: Weinheim, 2011; pp 19

(15) Mayor, M.; Weber, H. B.; Reichert, J.; Elbing, M.; von Hänish, C.; Beckmann, D.; Fischer, M. *Angew. Chem., Int. Ed.* **2003**, *42*, 5834.

(16) Fracasso, D.; Valkenier, H.; Hummelen, J. C.; Solomon, G. C.; Chiechi, R. C. *J. Am. Chem. Soc.* **2011**, *133*, 9556.

(17) Guédon, C. M.; Valkenier, H.; Markussen, T.; Thygesen, K. S.; Hummelen, J. C.; van der Molen, S. J. *Nat. Nanotechnol.* **2012**, *7*, 305.

(18) Darwish, N.; Díez-Pérez, I.; Da Silva, P.; Tao, N.; Gooding, J. J.; Paddon-Row, M. N. *Angew. Chem., Int. Ed.* **2012**, *51*, 3203.

(19) Ballmann, S.; Härtle, R.; Coto, P. B.; Elbing, M.; Mayor, M.; Bryce, M. R.; Thoss, M.; Weber, H. B. *Phys. Rev. Lett.* **2012**, *109*, 056801.

(20) Aradhya, S. V.; Meisner, J. S.; Krikorian, M.; Ahn, S.; Parameswaran, R.; Steigerwald, M. L.; Nuckolls, C.; Venkataraman, L. *Nano Lett.* **2012**, *12*, 1643.

(21) Park, H.; Lim, A. K. M.; Alivisatos, A. P.; Park, J.; McEuen, P. L. *Appl. Phys. Lett.* **1999**, *75*, 301.

(22) O'Neill, K.; Osorio, E. A.; van der Zant, H. S. J. *Appl. Phys. Lett.* **2007**, *90*, 133109.

(23) Mangin, A.; Anthore, A.; Della Rocca, M. L.; Boulat, E.; Lafarge, P. *J. Appl. Phys.* **2009**, *105*, 014313.

(24) Van Ruitenbeek, J. M.; Alvarez, A.; Pineyro, I.; Grahmann, C.; Joyez, P.; Devoret, M. H.; Esteve, D.; Urbina, C. *Rev. Sci. Instrum.* **1996**, *67*, 108.

(25) Kergueris, C.; Bourgoin, J. P.; Palacin, S.; Esteve, D.; Urbina, C.; Magoga, M.; Joachim, C. *Phys. Rev. B* **1999**, *59*, 12505.

(26) (a) Janin, M.; Ghilane, J.; Randriamahazake, H.; Lacroix, J. C. *Anal. Chem.* **2011**, *83*, 9709. (b) Janin, M.; Ghilane, J.; Lacroix, J. C. *J. Am. Chem. Soc.* **2013**, *135*, 2108.

(27) Sayed, S. Y.; Fereiro, J. A.; Yan, H.; McCreery, R. L.; Bergren, A. J. *Proc. Natl. Acad. Sci. U.S.A.* **2012**, *109*, 11498.

(28) Martin, P.; Della Rocca, M. L.; Anthore, A.; Lafarge, P.; Lacroix, J. C . *J. Am. Chem. Soc.* **2012**, *134*, 154.

(29) Kullapere, M.; Marandi, M.; Sammelselg, V.; Menezes, H. A.; Maia, G.; Tammeveski, K. *Electrochem. Commun.* **2009**, *11*, 405.

(30) Bousquet, A.; Ceccato, M.; Hinge, M.; Pedersen, S. U.; Daasbjerg, K. *Langmuir* **2012**, *28*, 1267. Stockhausen, V.; Ghilane, J.; Martin, P.; Trippé-Allard, G.; Randriamahazaka, H.; Lacroix, J. C. *J. Am. Chem. Soc.* **2009**, *131*, 14920.

(31) Stockhausen, V.; Ghilane, J.; Martin, P.; Trippé-Allard, G.; Randriamahazaka, H.; Lacroix, J. C. *J. Am. Chem. Soc.* **2009**, *131*, 14920.

(32) Santos, L.; Ghilane, J.; Martin, P.; Lacaze, P. C.; Randriamahazaka, H.; Lacroix, J.-C. *J. Am. Chem. Soc.* **2010**, *132*, 1690.

(33) Anariba, F.; DuVall, S. H.; McCreery, R. L. *Anal. Chem.* **2003**, *75*, 3837.

(34) Andrews, D. Q.; Solomon, G. C.; Van Duyne, R. P.; Ratner, M. A. *J. Am. Chem. Soc.* **2008**, *130*, 17309.

(35) Simmons, J. G. *J. Appl. Phys.* **1963**, *34*, 1793.

(36) Stratton, R. *J. Phys. Chem. Solids* **1962**, *23*, 1177.

(37) Ingold, G. L.; Nazarov, Y. V. In *Single Charge Tunneling: Coulomb Blockade Phenomena in Nanostructures*; Grabert, H., Devoret, M. H., Eds.; Plenum Press: New York, 1992.

(38) Härtle, R.; Butzin, M.; Rubio-Pons, O.; Thoss, M. *Phys. Rev. Lett.* **2011**, *107*, 046802.

(39) Osorio, E. A.; O'Neill, K.; Stuhr-Hansen, N.; Nielsen, O. F.; Bjørnholm, T.; van der Zant, H. S. J. *Adv. Mater.* **2007**, *19*, 281.